

RESIST LABEL NOISE WITH PGM FOR GRAPH NEURAL NETWORKS

Qingqing Ge¹, Jianxiang Yu¹, Zeyuan Zhao¹, Xiang Li¹

¹East China Normal University

{qingqingge, jianxiangyu, zeyuanzhao}@stu.ecnu.edu.cn

xiangli@dase.ecnu.edu.cn

ABSTRACT

While robust graph neural networks (GNNs) have been widely studied for graph perturbation and attack, those for label noise have received significantly less attention. Most existing methods heavily rely on the label smoothness assumption to correct noisy labels, which adversely affects their performance on heterophilous graphs. Further, they generally perform poorly in high noise-rate scenarios. To address these problems, in this paper, we propose a novel probabilistic graphical model (PGM) based framework LNP. Given a noisy label set and a clean label set, our goal is to maximize the likelihood of labels in the clean set. We first present LNP-v1, which generates clean labels based on graphs only in the Bayesian network. To further leverage the information of clean labels in the noisy label set, we put forward LNP-v2, which incorporates the noisy label set into the Bayesian network to generate clean labels. The generative process can then be used to predict labels for unlabeled nodes. We conduct extensive experiments to show the robustness of LNP on varying noise types and rates, and also on graphs with different heterophilies. In particular, we show that LNP can lead to inspiring performance in high noise-rate situations.

1 INTRODUCTION

Graph Neural Networks (GNNs) have been widely applied in a variety of fields, such as social network analysis Hamilton et al. (2017), drug discovery Li et al. (2021a), financial risk control Wang et al. (2019), and recommender systems Wu et al. (2022). However, real-world graph data often contain noisy labels, which are generally derived from inadvertent errors in manual labeling on crowdsourcing platforms or incomplete and inaccurate node features corresponding to labels. These noisy labels have been shown to degenerate the performance of GNNs Zhang et al. (2021); Patrini et al. (2017) and further reduce the reliability of downstream graph analytic tasks. Therefore, tackling label noise for GNNs is a critical problem to be addressed.

Recently, label noise has been widely studied in the field of Computer Vision (CV) Cheng et al. (2020); Yi et al. (2022); Han et al. (2018); Li et al. (2020); Shu et al. (2019), which aims to derive robust neural network models. Despite the success, most existing methods cannot be directly applied to graph-structured data due to the inherent non-Euclidean characteristics and structural connectivity of graphs. Although some methods specifically designed for graphs have shown promising results Nt et al. (2019); Li et al. (2021b); Du et al. (2021); Dai et al. (2021); Xia et al. (2021a); Qian et al. (2023), they still suffer from two main limitations. First, most existing approaches heavily rely on label smoothness to correct noisy labels, which assumes that neighboring nodes in a graph tend to have the same label. This assumption is typically used to express local continuity in homophilous graphs and does not hold in heterophilous graphs. When applied in graphs with heterophily, the performance of these methods could be significantly degraded. Second, while probabilistic graphical models have been successively used to handle label noise in CV, there remains a gap in applying them for GNNs against noisy labels. It is well known that probabilistic graphical model and Bayesian framework can model uncertainty and are thus less sensitive to data noise. Therefore, there arises a question: *Can we develop a probabilistic graphical model for robust GNNs resist noisy labels?*

In this paper, we study robust GNNs from a Bayesian perspective. Since it is generally easy to obtain an additional small set of clean labels at low cost, we consider a problem scenario that includes both a noisy training set and a clean one of much smaller size. We propose a novel Label Noise-resistant framework based on Probabilistic graphical model for GNNs, namely, *LNP*. We emphasize that LNP does not assume label smoothness, and can be applied in both graphs with homophily and heterophily. Given a noisy label set Y_N and a much smaller clean label set Y_C in a graph G , our goal is to maximize the likelihood of clean labels in Y_C . To reduce the adverse effect from noise in Y_N , LNP-v1 (version 1) maximizes $P(Y_C|G)$, which assumes the conditional dependence of Y_C on G only in the Bayesian network. Specifically, LNP-v1 first introduces a hidden variable \bar{Y} that expresses noisy labels for nodes, and then generates clean labels Y_C based on both G and \bar{Y} . Note that LNP-v1 implicitly restricts the closeness between \bar{Y} and Y_N to take advantage of informative clean labels in Y_N . To better use Y_N , we further present LNP-v2 (version 2), which assumes the conditional dependence of Y_C on both G and Y_N , and maximizes $P(Y_C|G, Y_N)$. The simultaneous usage of G and Y_N can lead to less noisy \bar{Y} and further improves the accuracy of Y_C generation. To maximize the likelihood, we employ the variational inference framework and derive ELBOs as objectives in both LNP-v1 and LNP-v2. In particular, we use three independent GNNs to implement the encoder that generates \bar{Y} , the decoder that generates Y_C , and the prior knowledge of \bar{Y} , respectively. Since node raw features and labels in Y_C or Y_N could be in different semantic space, directly concatenating features with one-hot encoded labels as inputs of GNNs could result in undesired results. To solve the issue, we first perform GNNs on raw features to generate node embeddings, based on which label prototype vectors are then calculated. In this way, node features and labels can be inherently mapped into the same low-dimensional space. After that, we fuse node embeddings and label prototype vectors to generate both \bar{Y} and Y_C . During the optimization, we highlight clean labels while attenuating the adverse effect of noisy labels in Y_N . Finally, we summarize our main contributions in this paper as:

- We propose LNP, which is the first probabilistic graphical model based framework for robust GNNs resist noisy labels, to our best knowledge.
- We disregard the label smoothness assumption for noise correction, which leads to the wide applicability of LNP in both homophilous and heterophilous graphs.
- We extensively demonstrate the effectiveness of LNP on different benchmark datasets, GNN architectures, and various noise types and rates. In particular, we show that LNP can lead to inspiring performance in high noise-rate situations.

2 RELATED WORK

2.1 DEEP NEURAL NETWORKS WITH NOISY LABELS

Learning with noisy labels has been widely studied in CV. From Song et al. (2022), most existing methods can be summarized in the following five categories: Robust architecture Cheng et al. (2020); Yao et al. (2018); Robust regularization Yi et al. (2022); Xia et al. (2021b); Wei et al. (2021); Robust loss function Ma et al. (2020); Zhang & Sabuncu (2018); Loss adjustment Huang et al. (2020); Wang et al. (2020b); Sample selection Han et al. (2018); Yu et al. (2019b); Li et al. (2020); Wei et al. (2020). However, the aforementioned approaches are dedicated to identically distributed (i.i.d) data, which may not be directly applicable to GNNs for handling noisy labels because the noisy information can propagate via message passing of GNNs.

2.2 ROBUST GRAPH NEURAL NETWORKS

In recent years, GNN has gained significant attention due to its broad range of applications in downstream tasks, such as node classification Oono & Suzuki (2019), link prediction Baek et al. (2020), graph classification Errica et al. (2019), and feature reconstruction Hou et al. (2022). Generally, existing robust GNN methods can be mainly divided into two categories: one that deals with perturbed graph structures and node features Zhu et al. (2021); Zhang & Zitnik (2020); Yu et al. (2021); Wang et al. (2020a), while the other that handles noisy labels. In this paper, we focus on solving the problem of the latter and only few works have been proposed. For example, D-GNN Nt et al. (2019) applies the backward loss correction to reduce the effects of noisy labels. UnionNET Li et al. (2021b) performs label aggregation to estimate node-level class probability distributions, which are

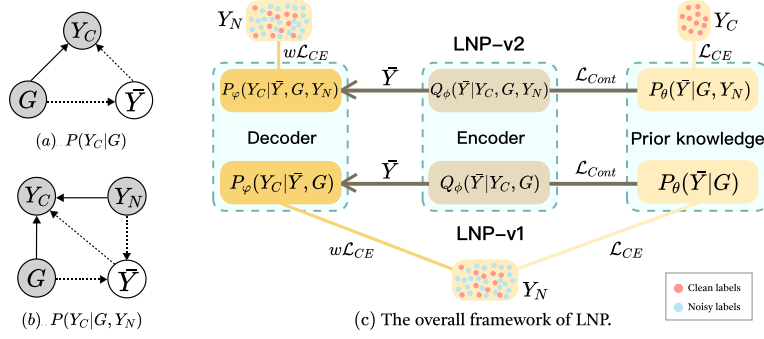


Figure 1: Bayesian networks of (a) $P(Y_C|G)$ and (b) $P(Y_C|G, Y_N)$. Here, G is the input graph data, Y_C is the clean label set, Y_N is the noisy label set, and \bar{Y} is the hidden variable. Arrows with solid lines and dashed lines denote generative process and inference process, respectively.

used to guide sample reweighting and label correction. PIGNN Du et al. (2021) leverages the PI (Pairwise Interactions) between nodes to explicitly adjust the similarity of those node embeddings during training. To alleviate the negative effect of the collected sub-optimal PI labels, PIGNN further introduces a new uncertainty-aware training approach and reweights the PI learning objective by its prediction confidence. NRGNN Dai et al. (2021) connects labeled nodes with high similarity and unlabeled nodes, constructing a new adjacency matrix to train more accurate pseudo-labels. LPM Xia et al. (2021a) computes pseudo labels from the neighboring labels for each node in the training set using Label Propagation (LP) and utilizes meta learning to learn a proper aggregation of the original and pseudo labels as the final label. RTGNN Qian et al. (2023) is based on the hypothesis that clean labels and incorrect labels in the training set are given, which is generally difficult to satisfy in reality.

Despite their success, we observe that most of them heavily rely on the label smoothness assumption, so that they cannot be applied to heterophilous graphs. In addition, most of them perform poorly in high noise-rate. Different from these methods, our proposed method LNP can achieve superior performance under different noise types and rates on various datasets.

3 PRELIMINARY

We denote a graph as $G = (V, E)$, where $V = \{v_i\}_{i=1}^n$ is a set of nodes and $E \subseteq V \times V$ is a set of edges. Let A be the adjacency matrix of G such that A_{ij} represents the weight of edge e_{ij} between nodes v_i and v_j . For simplicity, we set $A_{ij} = 1$ if $e_{ij} \in E$; 0, otherwise. Nodes in the graph are usually associated with features and we denote X as the feature matrix, where the i -th row x_i indicates the feature vector of node v_i .

Definition 1 Given a graph G that contains a small clean training set \mathcal{T}_C with labels Y_C and a noisy training set \mathcal{T}_N with labels Y_N , where $|\mathcal{T}_C| \ll |\mathcal{T}_N|$, our task is to learn a robust GNN $f(\cdot)$ that can predict the labels Y_U of unlabeled nodes, i.e.,

$$f(G, \mathcal{T}_C, \mathcal{T}_N) \rightarrow Y_U. \quad (1)$$

4 METHODOLOGY

4.1 LNP-v1

To predict Y_U for unlabeled nodes, we need to calculate the posterior distribution $P(Y_U|G, Y_C, Y_N)$. Instead of calculating the posterior directly, we propose to maximize the likelihood of $P(Y_C|G)$, which aims to generate the informative clean labels Y_C . The generative process can then be used to predict Y_U . The Bayesian network for generating Y_C is shown in Figure 1(a) and the generative process is formulated as:

$$P(Y_C|G) = \int_{\bar{Y}} P(Y_C|\bar{Y}, G)P(\bar{Y}|G)d\bar{Y}. \quad (2)$$

Generally, the hidden variable \bar{Y} can be interpreted as node embedding matrix. Since the matrix is then used to predict node labels, we directly denote \bar{Y} as noisy label predictions for all the nodes in the graph. The generative process can be described as follows: we first obtain noisy label predictions \bar{Y} for all the nodes in the graph, and then jointly consider G and \bar{Y} to generate the true clean labels Y_C . Since directly optimizing $P(Y_C|G)$ is difficult, we introduce a variational distribution $Q_\phi(\bar{Y}|Y_C, G)$ with parameters ϕ and employ variational inference to derive the evidence lower bound (ELBO) as:

$$\log P_{\theta, \phi}(Y_C|G) \geq E_{Q_\phi(\bar{Y}|Y_C, G)} \log P_\phi(Y_C|\bar{Y}, G) - KL(Q_\phi(\bar{Y}|Y_C, G) || P_\theta(\bar{Y}|G)) = \mathcal{L}_{ELBO}^1. \quad (3)$$

Here, $Q_\phi(\bar{Y}|Y_C, G)$ characterizes the encoding (mapping) process, while $P_\phi(Y_C|\bar{Y}, G)$ represents the decoding (reconstruction) process. Note that P_ϕ can generate predicted labels \hat{Y} for all the nodes more than \hat{Y}_C . Further, $P_\theta(\bar{Y}|G)$ captures the prior knowledge. In our experiments, we use three independent GNNs to implement them with learnable parameters ϕ , φ and θ , respectively. However, the above generative process ignores the given noisy labels Y_N , while Y_N still contains many clean node labels that are informative. To further employ the useful information from Y_N , we first apply a standard multiclass softmax cross-entropy loss $\mathcal{L}_{CE}(P_\theta, Y_N)$ to incorporate Y_N into the prior knowledge $P_\theta(\bar{Y}|G)$. In addition to Y_C , for nodes with clean labels in Y_N , it is also expected that their reconstructed labels should be close to their ground-truth ones. However, clean node labels are unknown in Y_N . To address the problem, we use the similarity between Y_N and \hat{Y}_N , denoted as $w \in \mathbb{R}^{|Y_N|}$, to measure the degree to which a node label in Y_N is clean. Intuitively, for a labeled node v_i in the noisy training set, if its reconstructed label \hat{y}_i is similar as its label $y_i \in Y_N$, it is more likely that y_i is a clean label; otherwise not. After that, we adopt a weighted cross-entropy loss $w\mathcal{L}_{CE}(P_\phi, Y_N)$, which assigns large weights to clean nodes while attenuating the erroneous effects of noisy labels. In addition, to leverage the extra supervision information from massive unlabeled data, inspired by Wan et al. (2021), we add the contrastive loss $\mathcal{L}_{Cont}(Q_\phi, P_\theta)$ to maximize the agreement of predictions of the same node that are generated from $Q_\phi(\bar{Y}|Y_C, G)$ and $P_\theta(\bar{Y}|G)$. Due to the space limitation, we defer details on \mathcal{L}_{Cont} to the Appendix C. Finally, the overall loss function is formulated as:

$$\mathcal{L}_1(\theta, \varphi, \phi) = -\mathcal{L}_{ELBO}^1(\theta, \varphi, \phi) + \lambda_1 w\mathcal{L}_{CE}(P_\phi, Y_N) + \lambda_2 \mathcal{L}_{CE}(P_\theta, Y_N) + \lambda_3 \mathcal{L}_{Cont}(Q_\phi, P_\theta) \quad (4)$$

where λ_1 , λ_2 and λ_3 are hyper-parameters to balance the losses.

4.2 LNP-v2

In Section 4.1, LNP-v1 leverages Y_N from two aspects. On the one hand, Y_N is considered as the prior knowledge and incorporated into P_θ . On the other hand, for nodes with clean labels in Y_N , their predicted labels are enforced to be close to the clean ones. However, Y_N is not directly included in the generative process of Y_C (see Figure 1(a)), and Y_C is only determined by G and the hidden variable \bar{Y} . From Equation 4, we see that LNP-v1 implicitly restricts the closeness between \bar{Y} and Y_N with regularization terms. In this way, when the number of erroneous labels in Y_N is large, \bar{Y} will be noisy and further degrade the performance of generating Y_C . To address the problem, we propose LNP-v2, which is a probabilistic graphical model using Y_N to generate Y_C (see Figure 1(b)). The goal of LNP-v2 is to maximize $P(Y_C|G, Y_N)$. Similarly, we introduce a variational distribution $Q_\phi(\bar{Y}|Y_C, G, Y_N)$ and derive the ELBO as:

$$\begin{aligned} \log P_{\theta, \phi}(Y_C|G, Y_N) \\ \geq E_{Q_\phi(\bar{Y}|Y_C, G, Y_N)} \log P_\phi(Y_C|\bar{Y}, G, Y_N) - KL(Q_\phi(\bar{Y}|Y_C, G, Y_N) || P_\theta(\bar{Y}|G, Y_N)) = \mathcal{L}_{ELBO}^2. \end{aligned} \quad (5)$$

In our experiments, we also use three independent GNNs to implement P_θ , Q_ϕ and P_ϕ , respectively. Note that the prior knowledge $P_\theta(\bar{Y}|G, Y_N)$ is a conditional distribution based on G and Y_N , so \bar{Y} is easily to be adversely affected by the noise label in Y_N . To reduce noise in \bar{Y} , we explicitly use cross-entropy loss $\mathcal{L}_{CE}(P_\theta, Y_C)$ to force \bar{Y} to be close to Y_C ¹. Similar as Equation 4, we formulate the overall objective by further adding a weighted cross-entropy term and a contrastive loss term:

$$\mathcal{L}_2(\theta, \varphi, \phi) = -\mathcal{L}_{ELBO}^2(\theta, \varphi, \phi) + \lambda_1 w\mathcal{L}_{CE}(P_\phi, Y_N) + \lambda_2 \mathcal{L}_{CE}(P_\theta, Y_C) + \lambda_3 \mathcal{L}_{Cont}(Q_\phi, P_\theta). \quad (6)$$

¹We do not explicitly add the term in Equation 4 because Y_N is not used as a condition in P_θ .

Different from LNP-v1, LNP-v2 explicitly adds Y_N in the Bayesian network to generate Y_C . Instead of enforcing the closeness between \bar{Y} and Y_N , LNP-v2 leverages the power of GNNs to correct noise labels in Y_N and obtain a high-quality \bar{Y} , leading to better reconstruction of Y_C .

4.3 ENCODER

In the encoder, we generate the hidden variable \bar{Y} based on $Q_\phi(\bar{Y}|Y_C, G)$ or $Q_\phi(\bar{Y}|Y_C, G, Y_N)$. A naive solution is to use one-hot encoded embeddings for labels in Y_C and Y_N , and concatenate them with raw node features, which are further fed into GNNs to output \bar{Y} ². However, labels and raw node features may correspond to different semantic spaces, which could adversely affect the model performance. To solve the issue, we employ label prototype vectors to ensure that labels and nodes are embedded into the same low-dimensional space. Specifically, we first run a GNN model on G to generate node embeddings $H \in \mathbb{R}^{n \times c}$, where c is the number of labels and the i -th row in H indicates the embedding vector h_i for node v_i . After that, for the j -th label l_j , we compute its prototype vector r_j by averaging the embeddings of nodes labeled as l_j in the clean training set Y_C . Finally, node embeddings and label prototype vectors are fused to generate \bar{Y} .

For $Q_\phi(\bar{Y}|Y_C, G)$, given a node v_i , we summarize the process to generate \bar{y}_i as: (1) if $v_i \in \mathcal{T}_C$ & $y_i = l_j$, $\bar{y}_i = \frac{1}{2}(h_i + r_j)$; (2) otherwise, $\bar{y}_i = \frac{1}{2}(h_i + \bar{r}_i)$. Here, $\bar{r}_i = \arg \max_{r_j} h_i^T r_j$, which denotes the most similar label prototype vector to node v_i .

Similarly, for $Q_\phi(\bar{Y}|Y_C, G, Y_N)$, we also describe the process to generate \bar{y}_i for node v_i as: (1) if $v_i \in \mathcal{T}_C$ & $y_i = l_j$, $\bar{y}_i = \frac{1}{2}(h_i + r_j)$; (2) if $v_i \in \mathcal{T}_N$ & $y_i = l_j$, $\bar{y}_i = \frac{1}{2}[h_i + \alpha r_j + (1 - \alpha)\bar{r}_i]$; (3) otherwise, $\bar{y}_i = \frac{1}{2}(h_i + \bar{r}_i)$. In particular, \bar{r}_i is used to alleviate the adverse effect of noise labels for nodes in \mathcal{T}_N , and $\alpha = \text{cosine}(h_i, r_j)$ is employed to control the importance of r_j and \bar{r}_i .

Obviously, the more nodes in \mathcal{T}_C , the more accurate r will be. Therefore, in each training epoch, we expand \mathcal{T}_C by adding nodes from \mathcal{T}_N with high confidence. Specifically, for each node in \mathcal{T}_N , we measure the similarity between its predicted label and given label in Y_N . When the similarity is greater than a pre-set threshold δ , we add it to \mathcal{T}_C . Additionally, we reset \mathcal{T}_C in each epoch to avoid adding too many nodes with noisy labels.

4.4 DECODER

Although we use $P_\phi(Y_C|\bar{Y}, G)$ and $P_\phi(Y_C|\bar{Y}, G, Y_N)$ in the ELBOs (see Eqs. 3 and 4), the decoder P_ϕ can generate labels \hat{Y} for all the nodes in the graph. On the one hand, considering $P_\phi(\cdot|\bar{Y}, G)$, we reconstruct \hat{y}_i for node v_i by $\hat{y}_i = \frac{1}{2}(h_i + \hat{r}_i)$, where $\hat{r}_i = \sum_{j=1}^c \bar{y}_{ij} r_j$. Here, we aggregate all prototype vectors r_j with probability \bar{y}_{ij} as weight. On the other hand, for $P_\phi(\cdot|\bar{Y}, G, Y_N)$, Y_N is given as a known conditional. When reconstructing the label \hat{y}_i for a node $v_i \in \mathcal{T}_N$, we have to consider both the hidden variable \bar{y}_i and the given label y_i . When \bar{y}_i and y_i are similar, the given label is more likely to be a clean one; otherwise, not. Therefore, the process to reconstruct \hat{y}_i for node v_i is adjusted as $\hat{y}_i = \frac{1}{2}(h_i + \hat{r}_i)$: (1) if $v_i \in \mathcal{T}_N$, $\hat{r}_i = \sum_{j=1}^c (\beta y_{ij} + (1 - \beta)\bar{y}_{ij}) r_j$; (2) otherwise, $\hat{r}_i = \sum_{j=1}^c \bar{y}_{ij} r_j$. Note that $\beta = \text{cosine}(\bar{y}_i, y_i)$ measures the cosine similarity between \bar{y}_i and y_i , which aims to assign large (small) weights to clean (noisy) labels.

4.5 PRIOR KNOWLEDGE

Different from the vanilla VAE that uses $\mathcal{N}(0, 1)$ as the prior knowledge, in our framework, we instead use $P_\theta(\bar{Y}|G)$ and $P_\theta(\bar{Y}|G, Y_N)$. For the former, based on the input graph G , we can run GNNs to get node embeddings $H \in \mathbb{R}^{n \times c}$ and set $\bar{Y} = H$. For the latter, although Y_N contains noise, there still exist many informative clean labels that can be utilized. Specifically, for each label l_j , we first compute the corresponding prototype vector r_j by averaging the embeddings of nodes labeled as l_j in \mathcal{T}_N . Then we describe the prior knowledge of \bar{y}_i as: (1) if $v_i \in \mathcal{T}_N$ & $y_i = l_j$, $\bar{y}_i = \frac{1}{2}(h_i + r_j)$; (2) otherwise, $\bar{y}_i = h_i$.

²For simplicity, variance in the Gaussian distribution is assumed to be 0.

5 EXPERIMENTS

In this section, we evaluate the performance of LNP on 8 benchmark datasets. We compare methods on the node classification task with classification accuracy as the measure. The analysis on the time and space complexity of the model is included in Appendix G.

5.1 EXPERIMENTAL SETTINGS

Datasets. We evaluate the performance of LNP using eight benchmark datasets Sen et al. (2008); Pei et al. (2020); Lim et al. (2021), including homophilous graphs *Cora*, *CiteSeer*, *PubMed*, *ogbn-arxiv*, and heterophilous graphs *Chameleon*, *Actor*, *Squirrel*, *snap-patents*. Here, *ogbn-arxiv* and *snap-patents* are large-scale datasets while others are small-scale ones. Details on these graph datasets are shown in Appendix A. For small-scale datasets, we follow Xia et al. (2021a) to split the datasets into 4:4:2 for training, validation and testing, while for large-scale datasets, we use the same training/validation/test splits as provided by the original papers. For fairness, we also conduct experiments on *Cora*, *CiteSeer* and *PubMed* following the standard semi-supervised learning setting, where each class only have 20 labeled nodes.

Setup. To show the model robustness, we corrupt the labels of training sets with two types of label noises. **Uniform Noise:** The label of each sample is independently changed to other classes with the same probability $\frac{p}{c-1}$, where p is the noise rate and c is the number of classes. **Flip Noise:** The label of each sample is independently flipped to similar classes with total probability p . In our experiments, we randomly select one class as a similar class with equal probability. For small-scale datasets, following Xia et al. (2021a), we only use nearly 25 labeled nodes from the validation set as the clean training set \mathcal{T}_C , where each class has the same number of samples. For large-scale datasets, a clean label set of 25 nodes is too small, so we set the size to be 0.2% of the training set size. For fairness, we use the same backbone GCN for LNP and other baselines. Due to the space limitation, we move implementation setup to Appendix B.

Baselines. We compare LNP with multiple baselines using the same network architecture. These baselines are representative, which include **Base models:** GCN Kipf & Welling (2016) and H2GCN Zhu et al. (2020); **Robust loss functions against label noise:** GCE loss Zhang & Sabuncu (2018) and APL Ma et al. (2020); **Typical and effective methods in CV:** Co-teaching plus Yu et al. (2019a); **Methods that handle noisy labels on graphs:** D-GNN Nt et al. (2019), NRGNN Dai et al. (2021) and LPM Xia et al. (2021a). For those baselines that do not consider the clean label set (GCN, GCE loss, APL, Co-teaching plus, D-GNN, NRGNN), we finetune them on the initial clean set after the model has been trained on the noisy training set for a fair comparison.

5.2 NODE CLASSIFICATION RESULTS

We perform node classification task, and compare LNP-v1 and LNP-v2 with other baselines under two types of label noise and four different levels of noise rates to demonstrate the effectiveness of our methods. Table 1 and 2 summarize the performance results on 6 small-scale datasets, from which we observe:

- (1) Compared with the base model GCN, GCE and APL generally perform better. This shows the effectiveness of robust loss function. However, as the noise rate increases, their performance drops significantly. For example, with 80% uniform noise on *Cora*, their accuracy scores are around 0.6, while the best accuracy (LNP-v2) is 0.7598.
- (2) LNP clearly outperforms D-GNN, NRGNN and LPM in heterophilous graphs. For example, with 80% flip noise on *Chameleon*, the accuracy scores of D-GNN, NRGNN and LPM are 0.3667, 0.3610 and 0.3782, respectively, while the best accuracy score (LNP-v2) is 0.4342. This is because they heavily rely on the label smoothness assumption that does not hold in heterophilous graphs.
- (3) LNP-v2 generally performs better than LNP-v1 at high noise rates. For example, with 80% flip noise on *Cora* and *PubMed*, the accuracy scores of LNP-v1 are 0.6481 and 0.7255, while that of LNP-v2 are 0.6731 and 0.7597, respectively. This is because LNP-v1 maximizes $P(Y_C|G)$, which generates Y_C based on G only (see Figure 1(a)), and implicitly restricts the closeness between \bar{Y} and Y_N with regularization terms to employ the useful information from Y_N . In this way, when the number of erroneous labels in Y_N is large, \bar{Y} will be noisy and further degrade the performance

Table 1: Comparison with baselines in test accuracy (%) with *uniform noise* on *small-scale datasets*. The best and the runner-up results are highlighted in **bold** and underlined respectively.

Datasets	p	GCN	Coteaching+	GCE	APL	DGNN	NRGNN	LPM	LNP-v1	LNP-v2
Cora	0.2	86.07(0.13)	83.03(0.19)	85.10(0.09)	86.26(0.05)	87.20(0.97)	86.42(0.26)	87.46(0.11)	87.50(0.67)	87.53(0.38)
	0.4	82.48(0.14)	71.68(0.21)	82.89(0.07)	82.01(0.13)	83.69(0.74)	83.91(1.39)	83.95(0.15)	84.63(0.22)	84.83(1.03)
	0.6	75.88(0.15)	50.05(0.31)	76.16(0.15)	74.49(0.11)	80.00(1.35)	80.33(2.06)	79.66(0.22)	80.40(1.52)	81.36(1.37)
	0.8	58.81(0.22)	36.39(0.44)	60.43(0.21)	58.72(0.25)	72.07(1.81)	72.77(3.57)	63.38(0.27)	75.51(1.95)	75.98(1.85)
CiteSeer	0.2	76.24(0.07)	75.49(0.24)	76.54(0.09)	74.32(0.17)	76.19(0.63)	76.25(0.45)	77.07(0.06)	77.23(0.69)	77.01(0.43)
	0.4	73.42(0.21)	72.71(0.13)	74.06(0.18)	71.77(0.15)	75.62(1.24)	74.80(1.43)	75.19(0.15)	76.01(1.00)	76.13(0.58)
	0.6	68.13(0.19)	66.63(0.41)	69.18(0.24)	66.78(0.22)	72.79(0.98)	70.69(0.70)	70.05(0.11)	72.97(0.85)	73.28(0.37)
	0.8	56.12(0.28)	56.27(0.36)	58.48(0.31)	56.08(0.34)	65.20(1.69)	67.30(1.11)	61.71(0.22)	68.52(1.17)	67.51(1.56)
PubMed	0.2	86.17(0.13)	85.23(0.21)	86.11(0.14)	85.86(0.20)	86.93(0.20)	85.60(0.24)	86.18(0.15)	86.63(0.18)	86.01(0.16)
	0.4	85.00(0.26)	84.30(0.49)	85.16(0.32)	85.48(0.24)	85.70(0.21)	82.12(1.39)	86.01(0.24)	85.81(0.14)	85.85(0.21)
	0.6	83.95(0.44)	82.69(0.40)	83.99(0.67)	84.63(0.43)	84.62(0.25)	80.33(2.06)	84.17(0.07)	84.69(0.27)	84.32(0.37)
	0.8	81.75(0.69)	80.18(0.13)	81.89(0.67)	82.28(0.61)	82.41(0.68)	78.83(3.57)	82.08(0.96)	82.62(0.42)	82.38(0.52)
Chameleon	0.2	57.54(1.06)	56.67(1.43)	57.54(1.47)	58.99(1.15)	56.18(2.26)	50.70(1.13)	55.39(2.68)	60.03(1.68)	59.97(0.76)
	0.4	55.13(1.68)	53.90(4.24)	55.48(2.24)	56.18(1.45)	53.77(2.83)	44.78(1.33)	50.04(2.93)	57.88(2.43)	57.23(0.99)
	0.6	50.35(1.74)	49.78(1.90)	50.22(1.74)	49.96(1.70)	48.55(1.67)	40.48(4.66)	48.20(2.13)	51.89(2.22)	52.41(0.97)
	0.8	41.40(1.53)	41.36(3.66)	41.23(1.54)	40.79(2.11)	41.01(2.96)	35.22(2.99)	40.48(2.16)	44.87(3.40)	45.61(3.37)
Actor	0.2	31.50(0.45)	30.29(0.66)	31.54(0.54)	29.93(0.31)	31.46(0.53)	30.93(0.84)	28.97(2.09)	32.25(0.55)	32.10(0.29)
	0.4	31.13(0.48)	30.28(0.50)	30.88(0.40)	29.26(0.27)	30.49(1.29)	29.09(0.58)	27.63(2.09)	30.96(0.42)	31.08(0.39)
	0.6	30.03(0.85)	29.53(0.59)	30.05(0.68)	29.12(0.85)	29.92(0.86)	28.36(0.79)	27.58(1.36)	31.59(0.77)	32.84(0.61)
	0.8	28.70(0.78)	27.92(0.80)	28.71(0.94)	28.11(1.08)	28.07(0.51)	28.09(0.81)	26.89(0.32)	29.51(0.38)	30.92(0.23)
Squirrel	0.2	36.20(0.64)	35.93(3.08)	35.98(0.83)	32.24(4.39)	40.81(2.17)	32.51(0.92)	32.05(1.36)	39.48(0.57)	40.90(0.39)
	0.4	34.31(0.84)	35.49(1.41)	34.20(0.59)	31.99(2.58)	35.37(1.55)	31.57(1.91)	32.12(1.90)	37.60(0.85)	36.48(1.37)
	0.6	31.68(1.31)	32.93(1.37)	31.70(1.01)	29.55(0.58)	32.79(1.45)	30.49(1.27)	28.68(2.66)	33.06(0.83)	33.28(1.14)
	0.8	29.88(1.62)	30.82(1.36)	29.61(1.42)	28.61(1.01)	28.70(3.08)	28.57(1.26)	26.13(0.83)	31.68(0.94)	32.64(1.48)

Table 2: Comparison with baselines in test accuracy (%) with *flip noise* on *small-scale datasets*.

Datasets	p	GCN	Coteaching+	GCE	APL	DGNN	NRGNN	LPM	LNP-v1	LNP-v2
Cora	0.2	82.89(0.14)	81.37(0.21)	83.21(0.13)	82.70(0.79)	83.99(0.77)	85.09(0.43)	86.95(0.12)	86.87(0.57)	87.01(0.32)
	0.4	67.39(0.42)	53.00(0.51)	67.80(0.37)	65.00(1.73)	74.43(3.68)	71.51(3.26)	78.97(0.33)	80.02(1.57)	79.34(2.06)
	0.6	51.99(1.13)	48.97(9.05)	57.82(2.50)	59.19(4.25)	61.11(3.04)	64.58(4.83)	60.63(3.72)	69.69(1.46)	71.55(3.63)
	0.8	41.33(1.12)	47.56(2.80)	50.52(3.51)	50.96(2.58)	62.88(7.27)	55.76(8.12)	42.19(4.56)	64.81(1.61)	67.31(3.11)
CiteSeer	0.2	75.08(0.22)	74.66(0.21)	76.36(0.20)	73.38(0.13)	76.04(0.61)	76.91(0.18)	76.39(0.14)	76.98(0.38)	76.24(0.56)
	0.4	61.41(0.23)	60.59(0.33)	63.66(0.46)	60.81(0.52)	65.41(1.99)	64.95(1.33)	68.71(0.39)	71.68(1.06)	71.32(0.59)
	0.6	36.16(2.17)	52.01(3.13)	56.46(2.99)	58.79(4.94)	60.15(3.79)	56.40(6.75)	60.71(3.55)	67.80(1.33)	68.35(1.62)
	0.8	30.54(2.79)	31.23(7.26)	41.59(3.54)	42.97(6.09)	60.09(4.60)	47.67(7.12)	44.07(3.52)	64.58(2.10)	66.67(2.15)
PubMed	0.2	85.55(0.24)	84.61(0.22)	85.47(0.06)	85.52(0.06)	86.66(0.22)	81.95(0.09)	85.58(0.13)	85.70(0.10)	85.76(0.21)
	0.4	80.88(0.32)	73.99(0.33)	80.03(0.42)	70.08(0.16)	81.45(1.63)	75.89(0.39)	83.15(0.36)	83.32(0.32)	83.52(0.40)
	0.6	60.40(2.79)	58.27(11.61)	63.55(2.09)	65.75(3.50)	74.04(4.55)	61.31(2.06)	71.20(4.33)	77.60(2.73)	77.44(3.27)
	0.8	51.17(3.85)	44.22(5.58)	61.42(3.90)	63.96(2.98)	70.52(4.70)	58.19(3.57)	59.19(2.62)	72.55(2.41)	75.97(2.78)
Chameleon	0.2	58.73(0.09)	41.01(2.95)	58.68(0.60)	54.21(0.16)	57.32(1.54)	52.28(0.91)	55.75(2.06)	59.34(1.40)	59.42(1.63)
	0.4	53.51(0.52)	35.35(2.79)	53.68(0.51)	38.42(3.96)	47.11(2.06)	45.13(1.17)	49.47(3.42)	53.70(2.02)	53.76(2.83)
	0.6	44.17(2.95)	27.68(3.56)	43.99(1.02)	34.43(2.91)	39.87(2.44)	36.84(3.10)	42.52(2.92)	44.56(1.62)	45.35(1.31)
	0.8	37.85(2.10)	24.30(1.63)	38.03(3.56)	35.13(3.02)	36.67(3.98)	36.10(3.21)	37.82(6.41)	41.10(3.16)	43.42(2.05)
Actor	0.2	31.37(0.29)	30.14(0.45)	31.25(0.12)	29.66(0.44)	30.55(0.53)	27.92(0.29)	27.00(0.31)	31.75(1.39)	31.30(1.09)
	0.4	28.66(1.29)	27.87(0.64)	28.83(0.98)	26.50(0.16)	27.75(1.05)	26.42(0.98)	23.37(1.91)	29.55(0.81)	29.05(0.83)
	0.6	26.96(0.46)	25.74(1.62)	26.71(0.23)	26.66(0.77)	26.89(2.33)	25.00(1.14)	25.54(1.28)	28.54(0.94)	28.79(0.51)
	0.8	26.67(0.27)	26.92(0.73)	26.72(0.26)	26.55(0.79)	26.93(2.31)	23.57(0.97)	22.47(2.71)	28.50(0.86)	28.72(0.43)
Squirrel	0.2	35.97(0.28)	33.58(0.52)	35.77(0.43)	26.01(3.52)	40.00(0.77)	33.14(2.14)	32.28(0.78)	41.28(0.37)	40.73(0.62)
	0.4	31.74(0.34)	30.26(2.66)	31.51(0.57)	24.57(1.23)	34.31(1.76)	31.35(1.47)	28.45(1.35)	37.21(1.25)	36.50(1.82)
	0.6	28.01(0.80)	26.86(1.17)	28.59(0.83)	24.03(1.33)	29.97(1.02)	28.17(1.71)	25.96(2.30)	33.05(0.93)	33.72(1.01)
	0.8	26.32(0.97)	25.65(2.12)	25.98(1.53)	23.90(0.78)	28.36(2.01)	26.95(1.00)	22.44(2.44)	31.84(0.49)	32.22(0.82)

of generating Y_C . However, LNP-v2 maximizes $P(Y_C|G, Y_N)$, directly incorporating Y_N in the Bayesian network to generate Y_C (see Figure 1(b)). In particular, when generating \bar{Y} , LNP-v2 can leverage the power of GNNs to correct noise labels in Y_N and obtain a high-quality \bar{Y} , which leads to better reconstruction of Y_C .

(4) LNP achieves the best or runner-up performance in all 48 cases. This shows that it can consistently provide superior results on datasets in a wide range of diversity. On the one hand, LNP disregards the label smoothness assumption for noise correction, which leads to its wide applicability in both homophilous and heterophilous graphs. On the other hand, LNP is modeled based on probabilistic graphical model and Bayesian framework, which can model uncertainty and are thus less sensitive to data noise.

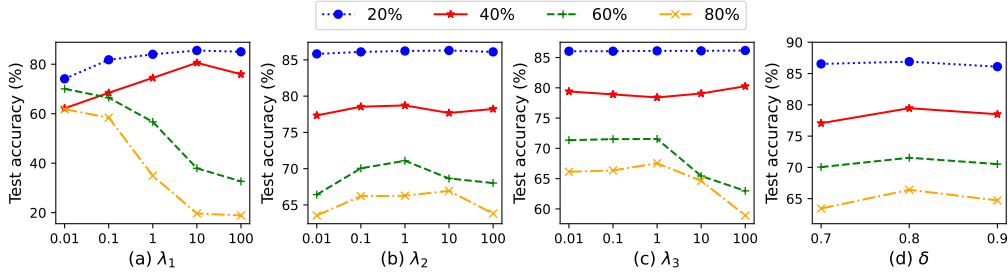


Figure 2: Hyper-parameter sensitivity analysis

For experiments on the large-scale datasets and in the standard semi-supervised learning setting, we observe similar results as above. Therefore, due to the space limitation, we move the corresponding results to Appendix D and E, respectively.

5.3 HYPER-PARAMETER SENSITIVITY ANALYSIS

We further perform a sensitivity analysis on the hyper-parameters of our method LNP-v2. In particular, we study four key hyper-parameters: the weights for three additional losses besides ELBO, λ_1 , λ_2 , λ_3 , representing the importance of $w\mathcal{L}_{CE}(P_\phi, Y_N)$, $\mathcal{L}_{CE}(P_\theta, Y_N)$ and $\mathcal{L}_{Cont}(Q_\phi, P_\theta)$ respectively, and the threshold δ that controls whether nodes can add to \mathcal{T}_C . In our experiments, we vary one parameter each time with others fixed. Figure 2 illustrates the results under flip noise ranging from 20% to 80% on Cora. From the figure, we see that

(1) As λ_1 increases, LNP-v2 achieves better performance in low noise-rate while achieving worse performance in high noise-rate. This is because there are many incorrect labels in Y_N when the noise rate is high, which may play a great role in misleading the reconstruction of Y_C . (2) Under high noise rates, LNP-v2 performs poorly when λ_2 is too small ($\lambda_2 = 0.01$) or too large ($\lambda_2 = 100$). This is due to the fact that when λ_2 is too small, the prior knowledge fails to provide effective positive guidance, while when λ_2 is too large, the potential erroneous information contained in the prior knowledge can have a detrimental effect and lead to a decrease in performance. (3) Although the test accuracy decreases when λ_3 is set large in high noise rates, LNP-v2 can still give stable performances over a wide range of parameter values from $[0.01, 1]$. (4) As δ increases, the test accuracy first increases and then decreases. This is because when δ is small, a lot of noise-labeled nodes will be added to \mathcal{T}_C , and when δ is large, more clean-labeled nodes will not be added to \mathcal{T}_C , resulting in a large deviation in the prototype vector, which will cause poor performance.

5.4 ABLATION STUDY

We conduct an ablation study on LNP-v2 to understand the characteristics of its main components. One variant does not consider the useful information from Y_N , training the model without $\mathcal{L}_{CE}(P_\phi, Y_N)$. We call this variant **LNP-nl** (no $\mathcal{L}_{CE}(P_\phi, Y_N)$). Another variant training the model without $\mathcal{L}_{CE}(P_\theta, Y_C)$, which helps us understand the importance of introducing prior knowledge. We call this variant **LNP-np** (no prior knowledge). To show the importance of the contrastive loss, we train the model without $\mathcal{L}_{Cont}(P_\theta, Y_C)$ and call this variant **LNP-nc** (no contrastive loss). Moreover, we consider a variant of LNP-v2 that applies $\mathcal{L}_{CE}(P_\theta, Y_N)$ directly, without weight w . We call this variant **LNP-nw** (no weight). Finally, we ignore the problem of semantic space inconsistency between variables, directly concatenating features with one-hot encoded labels as inputs of GNNs. This variant helps us evaluate the effectiveness of introducing label prototype vectors to generate \bar{Y} and Y_C . We call this variant **LNP-nv** (no prototype vectors). We compare LNP-v2 with these variants in the 80% noise rate on all datasets. The results are given in Figure 3. From it, we observe:

(1) LNP-v2 beats LNP-nl in all cases. This is because Y_N contains a portion of clean labels, which can well guide the reconstruction of Y_C . (2) LNP-v2 achieves better performance than LNP-np. This further shows the importance of using Y_C to guide prior knowledge. (3) LNP-v2 performs better than LNP-nc. This shows that the contrastive loss can leverage the extra supervision information from massive unlabeled data and maximize the agreement of node predictions generated

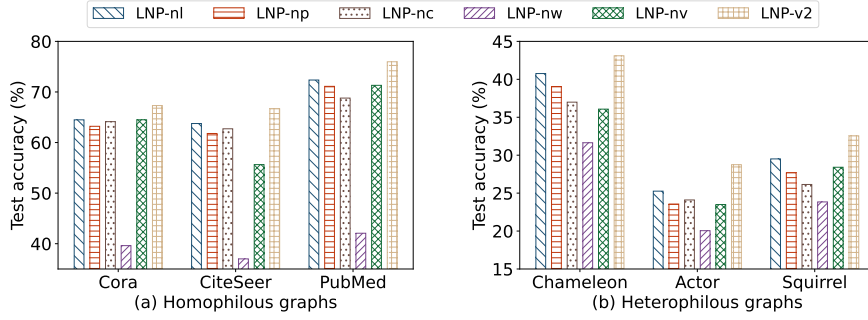


Figure 3: The ablation study results on six datasets with 80% flip noise.

from $Q_\phi(\bar{Y}|Y_C, G, Y_N)$ and $P_\theta(\bar{Y}|G, Y_N)$. **(4)** LNP-v2 clearly outperforms LNP-nw in all datasets. LNP-nw, which ignores the noisy labels in Y_N , directly applies cross-entropy loss between the reconstructed labels and Y_N . Since there are many incorrect labels in Y_N , it will negatively affect the reconstructed labels. **(5)** LNP-v2 outperforms LNP-nv. This shows the effectiveness of mapping node features and labels into the same low-dimensional space instead of directly concatenating features with one-hot encoded labels as inputs of GNNs.

5.5 STUDY ON THE SIZE OF THE CLEAN LABEL SET

We next study the sensitivity of LNP on the size of the clean label set. As can be seen in Figure 4(a), our method can achieve very stable performance over a wide range of set sizes on both CiteSeer (homophilous graph) and Chameleon (heterophilous graph) in various noise rates. Given only 20 clean labels, LNP can perform very well. With the increase of the clean set size, there only brings marginal improvement on the test accuracy. This further shows that the problem scenario we set is meaningful and feasible. We only need to obtain an additional small set of clean labels at low cost to achieve superior results. We also evaluate the robustness of LNP against other baselines w.r.t. the clean label set size. Figure 4(b) shows the results with 80% flip noise. From the figure, we observe that LNP consistently outperforms other baselines in all cases, which further verifies the robustness of LNP.

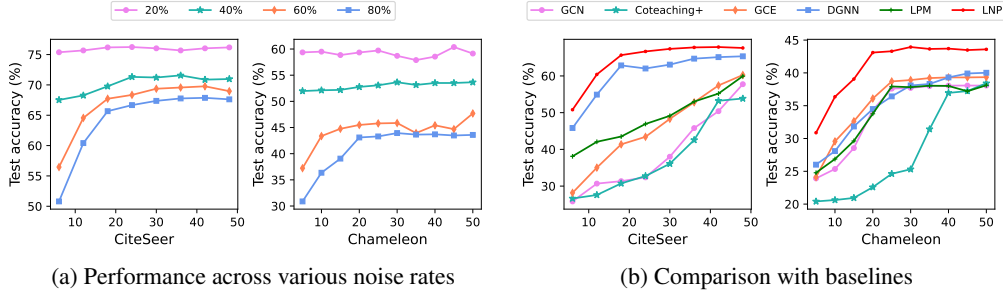


Figure 4: Robustness study of LNP w.r.t. the clean label set size

6 CONCLUSION

In this paper, we proposed LNP, which is the first probabilistic graphical model based framework for robust GNNs resist noisy labels. It disregards the label smoothness assumption and can be applied in both graphs with homophily and heterophily. We first maximized $P(Y_C|G)$ and employed Y_N in regularization terms only. To further leverage clean labels in Y_N , we incorporated Y_N in the Bayesian network to generate Y_C and maximized $P(Y_C|G, Y_N)$. We also used label prototype vectors to ensure that labels and nodes are embedded into the same low-dimensional space. Finally, we conducted extensive experiments to show that LNP achieves robust performance under different noise types and rates on various datasets.

REFERENCES

- Jinheon Baek, Dong Bok Lee, and Sung Ju Hwang. Learning to extrapolate knowledge: Transductive few-shot out-of-graph link prediction. *Advances in Neural Information Processing Systems*, 33:546–560, 2020.
- Lele Cheng, Xiangzeng Zhou, Liming Zhao, Dangwei Li, Hong Shang, Yun Zheng, Pan Pan, and Yinghui Xu. Weakly supervised learning with side information for noisy labeled images. In *Computer Vision–ECCV 2020: 16th European Conference, Glasgow, UK, August 23–28, 2020, Proceedings, Part XXX 16*, pp. 306–321. Springer, 2020.
- Enyan Dai, Charu Aggarwal, and Suhang Wang. Nrgnn: Learning a label noise resistant graph neural network on sparsely and noisily labeled graphs. In *Proceedings of the 27th ACM SIGKDD Conference on Knowledge Discovery & Data Mining*, pp. 227–236, 2021.
- Xuefeng Du, Tian Bian, Yu Rong, Bo Han, Tongliang Liu, Tingyang Xu, Wenbing Huang, and Junzhou Huang. Pi-gnn: A novel perspective on semi-supervised node classification against noisy labels. *arXiv preprint arXiv:2106.07451*, 2021.
- Federico Errica, Marco Podda, Davide Bacciu, and Alessio Micheli. A fair comparison of graph neural networks for graph classification. *arXiv preprint arXiv:1912.09893*, 2019.
- Will Hamilton, Zhitaoying, and Jure Leskovec. Inductive representation learning on large graphs. *Advances in neural information processing systems*, 30, 2017.
- Bo Han, Quanming Yao, Xingrui Yu, Gang Niu, Miao Xu, Weihua Hu, Ivor Tsang, and Masashi Sugiyama. Co-teaching: Robust training of deep neural networks with extremely noisy labels. *Advances in neural information processing systems*, 31, 2018.
- Zhenyu Hou, Xiao Liu, Yukuo Cen, Yuxiao Dong, Hongxia Yang, Chunjie Wang, and Jie Tang. Graphmae: Self-supervised masked graph autoencoders. In *Proceedings of the 28th ACM SIGKDD Conference on Knowledge Discovery and Data Mining*, pp. 594–604, 2022.
- Lang Huang, Chao Zhang, and Hongyang Zhang. Self-adaptive training: beyond empirical risk minimization. *Advances in neural information processing systems*, 33:19365–19376, 2020.
- Thomas N Kipf and Max Welling. Semi-supervised classification with graph convolutional networks. *arXiv preprint arXiv:1609.02907*, 2016.
- Junnan Li, Richard Socher, and Steven CH Hoi. Dividemix: Learning with noisy labels as semi-supervised learning. *arXiv preprint arXiv:2002.07394*, 2020.
- Pengyong Li, Jun Wang, Yixuan Qiao, Hao Chen, Yihuan Yu, Xiaojun Yao, Peng Gao, Guotong Xie, and Sen Song. An effective self-supervised framework for learning expressive molecular global representations to drug discovery. *Briefings in Bioinformatics*, 22(6):bbab109, 2021a.
- Yayong Li, Jie Yin, and Ling Chen. Unified robust training for graph neural networks against label noise. In *Advances in Knowledge Discovery and Data Mining: 25th Pacific-Asia Conference, PAKDD 2021, Virtual Event, May 11–14, 2021, Proceedings, Part I*, pp. 528–540. Springer, 2021b.
- Derek Lim, Felix Hohne, Xiuyu Li, Sijia Linda Huang, Vaishnavi Gupta, Omkar Bhalerao, and Ser Nam Lim. Large scale learning on non-homophilous graphs: New benchmarks and strong simple methods. *Advances in Neural Information Processing Systems*, 34:20887–20902, 2021.
- Xingjun Ma, Hanxun Huang, Yisen Wang, Simone Romano, Sarah Erfani, and James Bailey. Normalized loss functions for deep learning with noisy labels. In *International conference on machine learning*, pp. 6543–6553. PMLR, 2020.
- H. Nt, C. J. Jin, and T. Murata. Learning graph neural networks with noisy labels. 2019.
- Kenta Oono and Taiji Suzuki. Graph neural networks exponentially lose expressive power for node classification. *arXiv preprint arXiv:1905.10947*, 2019.

- Giorgio Patrini, Alessandro Rozza, Aditya Krishna Menon, Richard Nock, and Lizhen Qu. Making deep neural networks robust to label noise: A loss correction approach. In *Proceedings of the IEEE conference on computer vision and pattern recognition*, pp. 1944–1952, 2017.
- Hongbin Pei, Bingzhe Wei, Kevin Chen-Chuan Chang, Yu Lei, and Bo Yang. Geom-gcn: Geometric graph convolutional networks. *arXiv preprint arXiv:2002.05287*, 2020.
- Siyi Qian, Haochao Ying, Renjun Hu, Jingbo Zhou, Jintai Chen, Danny Z Chen, and Jian Wu. Robust training of graph neural networks via noise governance. In *Proceedings of the Sixteenth ACM International Conference on Web Search and Data Mining*, pp. 607–615, 2023.
- Prithviraj Sen, Galileo Namata, Mustafa Bilgic, Lise Getoor, Brian Galligher, and Tina Eliassi-Rad. Collective classification in network data. *AI magazine*, 29(3):93–93, 2008.
- Jun Shu, Qi Xie, Lixuan Yi, Qian Zhao, Sanping Zhou, Zongben Xu, and Deyu Meng. Meta-weight-net: Learning an explicit mapping for sample weighting. *Advances in neural information processing systems*, 32, 2019.
- Hwanjun Song, Minseok Kim, Dongmin Park, Yooju Shin, and Jae-Gil Lee. Learning from noisy labels with deep neural networks: A survey. *IEEE Transactions on Neural Networks and Learning Systems*, 2022.
- Sheng Wan, Yibing Zhan, Liu Liu, Baosheng Yu, Shirui Pan, and Chen Gong. Contrastive graph poisson networks: Semi-supervised learning with extremely limited labels. *Advances in Neural Information Processing Systems*, 34:6316–6327, 2021.
- Daixin Wang, Jianbin Lin, Peng Cui, Quanhui Jia, Zhen Wang, Yanming Fang, Quan Yu, Jun Zhou, Shuang Yang, and Yuan Qi. A semi-supervised graph attentive network for financial fraud detection. In *2019 IEEE International Conference on Data Mining (ICDM)*, pp. 598–607. IEEE, 2019.
- Xiao Wang, Meiqi Zhu, Deyu Bo, Peng Cui, Chuan Shi, and Jian Pei. Am-gcn: Adaptive multi-channel graph convolutional networks. In *Proceedings of the 26th ACM SIGKDD International conference on knowledge discovery & data mining*, pp. 1243–1253, 2020a.
- Zhen Wang, Guosheng Hu, and Qinghua Hu. Training noise-robust deep neural networks via meta-learning. In *Proceedings of the IEEE/CVF conference on computer vision and pattern recognition*, pp. 4524–4533, 2020b.
- Hongxin Wei, Lei Feng, Xiangyu Chen, and Bo An. Combating noisy labels by agreement: A joint training method with co-regularization. In *Proceedings of the IEEE/CVF conference on computer vision and pattern recognition*, pp. 13726–13735, 2020.
- Hongxin Wei, Lue Tao, Renchunzi Xie, and Bo An. Open-set label noise can improve robustness against inherent label noise. *Advances in Neural Information Processing Systems*, 34:7978–7992, 2021.
- Shiwen Wu, Fei Sun, Wentao Zhang, Xu Xie, and Bin Cui. Graph neural networks in recommender systems: a survey. *ACM Computing Surveys*, 55(5):1–37, 2022.
- Jun Xia, Haitao Lin, Yongjie Xu, Lirong Wu, Zhangyang Gao, Siyuan Li, and Stan Z Li. Towards robust graph neural networks against label noise. 2021a.
- Xiaobo Xia, Tongliang Liu, Bo Han, Chen Gong, Nannan Wang, Zongyuan Ge, and Yi Chang. Robust early-learning: Hindering the memorization of noisy labels. In *International conference on learning representations*, 2021b.
- Jiangchao Yao, Jiajie Wang, Ivor W Tsang, Ya Zhang, Jun Sun, Chengqi Zhang, and Rui Zhang. Deep learning from noisy image labels with quality embedding. *IEEE Transactions on Image Processing*, 28(4):1909–1922, 2018.
- Li Yi, Sheng Liu, Qi She, A Ian McLeod, and Boyu Wang. On learning contrastive representations for learning with noisy labels. In *Proceedings of the IEEE/CVF Conference on Computer Vision and Pattern Recognition*, pp. 16682–16691, 2022.

- Donghan Yu, Ruohong Zhang, Zhengbao Jiang, Yuexin Wu, and Yiming Yang. Graph-revised convolutional network. In *Machine Learning and Knowledge Discovery in Databases: European Conference, ECML PKDD 2020, Ghent, Belgium, September 14–18, 2020, Proceedings, Part III*, pp. 378–393. Springer, 2021.
- X. Yu, B. Han, J. Yao, G. Niu, Ivor W Tsang, and M. Sugiyama. How does disagreement help generalization against label corruption? 2019a.
- Xingrui Yu, Bo Han, Jiangchao Yao, Gang Niu, Ivor Tsang, and Masashi Sugiyama. How does disagreement help generalization against label corruption? In *International Conference on Machine Learning*, pp. 7164–7173. PMLR, 2019b.
- Chiyuan Zhang, Samy Bengio, Moritz Hardt, Benjamin Recht, and Oriol Vinyals. Understanding deep learning (still) requires rethinking generalization. *Communications of the ACM*, 64(3):107–115, 2021.
- Xiang Zhang and Marinka Zitnik. Gnn-guard: Defending graph neural networks against adversarial attacks. *Advances in neural information processing systems*, 33:9263–9275, 2020.
- Zhilu Zhang and Mert Sabuncu. Generalized cross entropy loss for training deep neural networks with noisy labels. *Advances in neural information processing systems*, 31, 2018.
- Jiong Zhu, Yujun Yan, Lingxiao Zhao, Mark Heimann, Leman Akoglu, and Danai Koutra. Beyond homophily in graph neural networks: Current limitations and effective designs. *Advances in Neural Information Processing Systems*, 33:7793–7804, 2020.
- Yanqiao Zhu, Weizhi Xu, Jinghao Zhang, Qiang Liu, Shu Wu, and Liang Wang. Deep graph structure learning for robust representations: A survey. *arXiv preprint arXiv:2103.03036*, 14, 2021.

A DATASETS

We summarize the statistics of the datasets used in experiments in Table 3.

Table 3: Statistics of the datasets.

Datasets	Cora	Citeseer	Pubmed	ogbn-arxiv	Chameleon	Actor	Squirrel	snap-patents
#Nodes	2,708	3,327	19,717	169,343	2,277	7,600	5,201	2,923,922
#Edges	5,278	4,552	44,324	1,166,243	31,421	26,752	198,493	13,975,788
#Features	1433	3703	500	128	2325	931	2089	269
#Classes	7	6	3	40	5	5	5	5

B IMPLEMENTATION DETAILS

We implement LNP with PyTorch and adopt the Adam optimizer to train the model. We perform a grid search to fine-tune hyper-parameters based on the results on the validation set. The search space of these hyper-parameters is listed in Table 4. Further, for other competitors (GCN, GCE, APL, Coteaching, LPM), some of their results are directly reported from Xia et al. (2021a) (Cora, CiteSeer with uniform noise ranging from 20% to 80% and Cora, CiteSeer, PubMed with flip noise ranging from 20% to 40%). For other cases, we fine-tune the model hyper-parameters with the codes released by their original authors. For fair comparison, we report the average results with standard deviations of 5 runs for all experiments. We run all the experiments on a server with 32G memory and a single Tesla V100 GPU.

Table 4: Grid search space.

Notation	Range
learning_rate	{1e-5, 1e-4, 1e-3, 1e-2}
weight_decay	{5e-5, 5e-4, 5e-3, 5e-2}
hidden_number	{32, 64, 128, 256}
dropout	[0.2, 0.8]
λ_1	{0.1, 0.5, 1, 1.5, 5, 10, 100}
λ_2	{0.1, 0.5, 1, 1.5, 5, 10, 100}
λ_3	{0.1, 0.5, 1, 1.5, 5, 10, 100}
δ	{0.7, 0.8, 0.9}

C DETAILS OF THE CONTRASTIVE LOSS

The contrastive loss \mathcal{L}_{Cont} is utilized to leverage the extra supervision information from massive unlabeled data. Specifically, taking LNP-v1 as an example, we maximize the agreement of predictions of the same node that are generated from $Q_\phi(\bar{Y}|Y_C, G)$ and $P_\theta(\bar{Y}|G)$. For notation simplicity, we denote the predictions as y_i and \tilde{y}_i for each node v_i , respectively. Meanwhile, we pull the predictions of different node pairs away. As a result, the pairwise contrastive loss between y_i and \tilde{y}_i can be defined as

$$\mathcal{L}_{PC}(y_i, \tilde{y}_i) = -\log \frac{\exp(\langle y_i, \tilde{y}_i \rangle / \tau)}{\exp(\langle y_i, \tilde{y}_i \rangle / \tau) + \sum_{j=1}^n \mathbb{1}_{[j \neq i]} \exp(\langle y_i, \tilde{y}_j \rangle / \tau) + \sum_{j=1}^n \mathbb{1}_{[j \neq i]} \exp(\langle y_i, y_j \rangle / \tau)} \quad (7)$$

where $\langle \cdot, \cdot \rangle$ denotes the inner product and τ is a temperature parameter. τ for LNP is set to be 0.5. Based on Equation 7, the overall contrastive objective to be minimized is

$$\mathcal{L}_{Cont} = \frac{1}{2n} \sum_{i=1}^n (\mathcal{L}_{PC}(y_i, \tilde{y}_i) + \mathcal{L}_{PC}(\tilde{y}_i, y_i)) \quad (8)$$

Table 5: Comparison with baselines in test accuracy (%) with *flip noise* on *large-scale datasets*.

Datasets	p	GCN	Coteaching+	GCE	APL	DGNN	NRGNN	LPM	LNP-v1	LNP-v2
ogbn-arxiv	0.2	54.73(0.28)	52.71(0.35)	55.22(0.29)	55.68(0.37)	53.49(0.48)	OOM	53.61(0.78)	56.40(0.39)	55.85(0.26)
	0.4	53.49(0.91)	50.12(0.83)	54.03(1.38)	53.79(0.62)	49.97(1.36)	OOM	48.83(0.82)	55.67(1.08)	54.82(0.85)
	0.6	35.01(1.03)	35.27(0.83)	36.71(0.79)	37.26(0.84)	32.90(0.95)	OOM	34.16(1.12)	41.75(1.14)	44.28(0.94)
	0.8	33.81(0.95)	31.65(1.27)	31.20(0.84)	35.27(0.81)	29.96(1.83)	OOM	35.63(0.84)	40.11(0.99)	42.39(0.74)
snap-patents	0.2	42.24(0.11)	41.55(0.18)	42.40(0.27)	42.36(0.19)	43.08(0.15)	OOM	39.62(0.32)	43.26(0.12)	43.05(0.11)
	0.4	36.23(0.29)	36.57(0.31)	36.29(0.25)	37.88(0.30)	37.06(0.62)	OOM	31.29(0.74)	39.32(0.26)	39.70(0.33)
	0.6	33.21(1.49)	31.55(1.98)	34.28(0.94)	34.05(1.27)	25.19(2.87)	OOM	28.11(3.65)	37.07(0.34)	38.01(0.81)
	0.8	32.57(1.74)	30.34(1.22)	31.90(0.78)	32.81(1.27)	23.25(2.99)	OOM	25.98(1.76)	36.75(1.53)	37.82(0.91)

D EXPERIMENTS ON LARGE-SCALE DATASETS

Table 5 summarizes the classification results on large-scale datasets. From the figure, we see that LNP consistently outperforms other baselines on both ogbn-arxiv (homophilous graph) and snap-patents (heterophilous graph). Further, when noise rates are high, the performance gap between LNP and baselines gets larger. This shows that LNP is more robust resist label noise. Further, since the edge prediction module in NRGNN has a time complexity of $O(n^2)$, it fails to run on large-scale datasets due to the out-of-memory (OOM) error.

E EXPERIMENTS IN THE STANDARD SEMI-SUPERVISED LEARNING SETTING

To further demonstrate the effectiveness of our methods, we perform node classification task, and compare LNP-v1 and LNP-v2 with other baselines in the standard semi-supervised learning setting where each class only have 20 labeled nodes for Cora, CiteSeer and PubMed. Table 6 summarizes the performance results, from which we observe that LNP clearly outperforms other baselines in all cases.

Table 6: Comparison with baselines in test accuracy (%) with *flip noise* and *standard semi-supervised learning setting*.

Datasets	p	Coteaching+	DGNN	NRGNN	LPM	LNP-v1	LNP-v2
Cora	0.2	72.55	78.65	78.14	77.27	80.30	<u>79.23</u>
	0.4	64.56	68.63	69.75	67.82	75.12	<u>72.68</u>
	0.6	55.12	63.38	62.52	60.93	<u>67.94</u>	69.00
	0.8	51.28	58.35	57.51	53.08	63.06	67.57
CiteSeer	0.2	58.43	62.42	64.36	63.29	<u>65.43</u>	66.63
	0.4	56.06	57.37	60.23	57.81	<u>61.86</u>	64.45
	0.6	50.18	53.15	54.35	52.03	<u>57.01</u>	61.31
	0.8	49.80	50.31	51.34	48.92	<u>52.25</u>	59.58
PubMed	0.2	72.26	75.32	74.93	75.02	76.84	<u>76.05</u>
	0.4	70.84	<u>74.10</u>	71.28	71.62	74.33	73.97
	0.6	69.38	71.92	70.37	70.18	<u>73.17</u>	73.23
	0.8	66.41	68.09	67.32	66.35	<u>71.34</u>	72.69

F LNP WITH H2GCN AS THE BACKBONE MODEL

Since our framework is flexible to use various GNNs as the backbone model, we also use two-layer H2GCN Zhu et al. (2020) for heterophilous graphs. Table 7 summarizes the performance results with flip noise. For fairness, we replace the corresponding backbones for other models except NRGNN and LPM, which are based on the assumption of label smoothness and can only use GCN as backbone. The results demonstrate that the performance of our proposed method LNP still leads other competitors.

Table 7: Comparison with baselines in test accuracy (%) on heterophilous graphs with *flip noise* and *H2GCN as the backbone GNN*.

Datasets	p	H2GCN	Coteaching+	GCE	APL	DGNN	NRGNN	LPM	LNP-v1	LNP-v2
Chameleon	0.2	55.44(0.90)	58.20(1.58)	56.75(1.19)	58.60(0.85)	51.54(1.49)	52.28(0.91)	55.75(2.06)	59.69(0.63)	59.34(0.61)
	0.4	50.04(2.03)	50.13(0.51)	51.23(2.48)	50.66(1.61)	44.17(3.97)	45.13(1.17)	49.47(3.42)	53.73(1.55)	52.76(1.62)
	0.6	42.48(3.16)	37.59(3.53)	42.84(2.45)	37.06(3.97)	34.61(2.24)	36.84(3.10)	42.52(2.92)	44.08(2.33)	43.05(2.47)
	0.8	37.95(2.58)	35.66(2.60)	38.01(3.15)	33.51(3.76)	32.24(1.57)	36.10(3.21)	37.82(6.41)	39.12(2.47)	38.10(2.35)
Actor	0.2	35.49(0.45)	35.78(0.94)	34.54(1.27)	33.78(0.76)	32.22(1.90)	27.92(0.29)	27.00(0.31)	35.82(1.48)	36.00(0.23)
	0.4	27.70(1.21)	32.01(0.93)	28.97(1.13)	28.34(1.31)	27.33(1.34)	26.42(0.98)	23.37(1.91)	32.79(1.04)	33.32(0.23)
	0.6	26.87(1.30)	29.28(1.87)	27.33(1.61)	26.09(0.44)	26.26(0.24)	25.00(1.14)	25.54(1.28)	31.17(1.62)	31.54(0.72)
	0.8	26.83(1.30)	27.84(1.32)	27.18(1.20)	24.51(2.82)	24.92(1.77)	23.57(0.97)	22.47(2.71)	29.93(2.87)	30.75(1.32)
Squirrel	0.2	43.30(0.91)	43.42(1.24)	42.44(1.04)	43.27(0.62)	39.21(0.61)	33.14(2.14)	32.28(0.78)	43.75(1.20)	43.90(1.29)
	0.4	36.10(1.01)	36.18(1.33)	34.66(1.59)	32.93(1.52)	28.93(2.04)	31.35(1.47)	28.45(1.35)	36.75(1.23)	36.41(0.99)
	0.6	32.33(3.37)	31.10(2.25)	32.22(3.17)	29.07(3.34)	25.40(2.11)	28.17(1.71)	25.96(2.30)	32.89(2.23)	33.09(2.19)
	0.8	27.30(4.12)	27.97(2.17)	26.34(3.91)	28.51(2.03)	25.21(0.74)	26.95(1.00)	22.44(2.44)	30.11(1.87)	31.54(0.61)

G TIME AND SPACE COMPLEXITY ANALYSIS

The major time complexity in the LNP comes from GNNs and the contrastive loss. Suppose we use one-layer GCN as the backbone. Since the adjacency matrix is generally sparse, let d_A be the average number of non-zero entries in each row of the adjacency matrix. Let n be the number of nodes, l be the raw features dimension, and c be the output layer dimension (c is the number of class labels). Further, let k be the number of selected negative samples. Then, the time complexities for GCN and the contrastive loss are $O(nd_A l + nlc)$ and $O(nkc)$, respectively, which are both linear to the number of nodes n .

For the space complexity, we need to store \bar{Y} whose size is nc (c is the number of class labels) and the parameters in GCN. Note that we use three independent GNNs in our framework. We still take one-layer GCN for illustration. For the convolutional layer in each GCN, there exists a learnable transformation matrix of size lc . Therefore, the overall space complexity is $O(nc + 3lc)$, which is also widely applicable.

We further conduct experiments to study model efficiency for different methods on two large-scale datasets. Note that we choose methods specially designed for graphs resist label noise for fair comparison and they all use GCN as the backbone model. We also take GCN as a reference model. We compare the convergence time (second) in training under flip noise rate = 0.8. We run all the experiments on one V100 GPU. Our results are shown in Table 8. From the table, we see that DGNN is very efficient. This is because based on GCN, DGNN only slightly adjusts the training objective by introducing a learnable noise correction matrix to the cross-entropy function. However, DGNN performs poorly under high noise rates. Further, our proposed methods are more efficient than NRGNN and LPM, which can also achieve the best classification performance (See Table 5). All these results show the superiority of our proposed methods.

Table 8: Comparison with baselines in convergence time (s) on large-scale datasets.

Datasets	GCN	DGNN	NRGNN	LPM	LNP-v1	LNP-v2
ogbn-arxiv	14.57	17.80	OOM	118.45	62.05	60.93
snap-patents	124.95	133.61	OOM	805.05	614.85	625.04

H LIMITATIONS

Although our methods solve the problem of noisy labels in both graphs with homophily and heterophily well, implementing them with three independent GNNs could be a drawback. How to implement our methods with less GNNs is a promising future research topic. Besides, experiments on datasets with real-world label noise are also needed to further show the effectiveness of LNP.